BBAA VI International Colloquium on:
Bluff Bodies Aerodynamics & Applications
Milano, Italy, July, 20-24 2008

FULL-SCALE IDENTIFICATION OF MODAL AND AEROELASTIC PARAMETERS OF THE CLIFTON SUSPENSION BRIDGE

Nikolaos Nikitas[*] , Jasna B. Jakobsen[†] and John H. G. Macdonald[*]

[*]Department of Civil Engineering
University of Bristol, University Walk, Bristol, BS8 1TR, UK
e-mails: N.Nikitas@bristol.ac.uk, John.Macdonald@bristol.ac.uk

[†]Department of Mechanical and Structural Engineering and Material Science
University of Stavanger, N-4036, Stavanger, Norway
e-mail: jasna.b.jakobsen@uis.no

Keywords: Full-scale, System identification, Ambient vibration data, Flutter derivatives.

Abstract. *Large-scale engineering structures subjected to severe wind loadings inherently suffer modelling uncertainties that can ultimately be validated in a full-scale testing process. Cases of structures which were found after construction to be operationally problematic is a common image in engineering history. Consequently full-scale analysis methods are quite important especially for monitoring existing structures, where revised designing trends and new building regulations cannot be taken into consideration. To this end we utilize a combination of conventional frequency based methods (for modal parameter extraction) together with a more elaborate stochastic identification technique (to retrieve flutter derivatives) for use with ambient vibration data collected during a testing series of the vibration response of the Clifton Suspension Bridge. Potentially unsafe behaviour during strong winds in the area is examined by analyzing the bridge dynamics. The outcome of this analysis provides a deeper insight into the bridge behaviour and shows the soundness of identification attempts with full-scale data, where randomness of wind excitation can raise validity issues.*

1 INTRODUCTION

For full-scale structures the most rational way to proceed with predictions of the reliability and operational safety includes identification methods from response only measurements. Especially for existing bridges, treatment of the flutter instability can substantially be verified this way. No analytical solutions exist for the bluff bodied irregular bridge cross-sections to prescribe the critical wind speed region so inevitably every investigation has to adopt some experimental or semi-empirical foundation to proceed on a further assessment. Thus most commonly wind tunnel tests on scaled models are used for reproducing the flutter phenomenon and it becomes evident that scaling issues may bring up inconsistencies, which can only be realized by analyzing the response of the real bridge. Additionally monitoring a structure's real response can reveal many aspects, which either due to modelling assumptions or to loading irregularities were concealed during the designing state.

For the current paper relating to the historic Clifton Suspension Bridge (CSB), shown in Fig. (1), a complete dynamic analysis from full-scale measurements is performed. The bridge cross-section, see Fig. (2), and the lightweight structure give rise to the need to examine the bridge's ability to cope with high winds. Indeed, on a few occasions in its 140 year lifetime large amplitude vibrations in strong winds have been reported. According to most empirical estimates of flutter speed, as in most bridge design rules, the CSB appears to be rather susceptible to wind-induced instabilities. Therefore even in moderate wind aeroelastic coupling of modes can become significant raising stability issues. For the current study we use the wind conditions and bridge response recordings of a period of four months, from November 2003 to March 2004. Available data include several periods of moderately strong winds, and reasonable ranges of wind speeds and directions, thus enabling a meaningful assessment of the wind contribution on the bridge dynamics.

The bridge span is 214m. Two ultrasonic anemometers were mounted 61m either side of midspan, more than 5m above road level. Nine servo-accelerometers were positioned along the bridge during an earlier analysis of the CSB dynamic response (see [1]). The positioning was selected such that the mode shapes could be identified. A near centre cross-section (27m from midspan) was picked to serve as the reference section by ensuring that all significant vibration modes could be measured there and the remaining accelerometers were arranged at a series of different cross-sections. Signals from all instruments were passed through anti-aliasing filters with a cut-off frequency of 4Hz, and were recorded at a sampling rate of 12.5Hz. The primary aims of this study were to determine i) the variation of modal characteristics with wind velocity ii) the effects of wind turbulence and vertical component of the wind iii) details of any large amplitude or other abnormal responses of the bridge.

Figure 1: Picture of the Clifton Suspension Bridge.

We herein use modal parameter estimates from a frequency based technique (for details on the procedure see [2]) together with a stochastic identification formulation especially modified to extract flutter derivatives, as described in [3]. Aeroelastic parameters have rarely been obtained from full-scale data. Jakobsen and Larose [4] addressed the problem and presented a comparative analysis with wind tunnel results. Costa and Borri [5] essentially applied the same identification routine, as described in [3] and [4], both on numerically simulated response and on real-scaled data, finding good quality performance of the method in every case. The existence of physical turbulence on site and the multi-modal behaviour of the bridge are characteristics that may explain the deviations from wind tunnel results. In this analysis due to lack of data from a scaled model, we use flutter derivatives of other bridge cross-sections, as presented by Scanlan and Tomko [6], to assess the self excited forces on the bridge response. Cross-sections employed for comparative purposes are chosen to represent both the low structural depth and the high parapets, perforated for the CSB, of the section in hand. Eventually for the CSB case study, a complete dynamic description is retrieved and questions on possible problematic performance are addressed.

Briefly the paper consists first of a short discussion on the acquired wind measurements. Typical wind speeds and wind turbulence conditions are described and the local terrain effects are addressed. Subsequently we move to the bridge response details. A conventional modal analysis is performed based on a linear modelling realization and all modal characteristics and their wind evolution are obtained. The last part containing the flutter derivative identification scheme first presents the employed Covariance Block Hankel Matrix (CBHM) formulation and subsequently the identification of the CSB case study. Conclusions on the method applicability and sensitivity complete the current presentation.

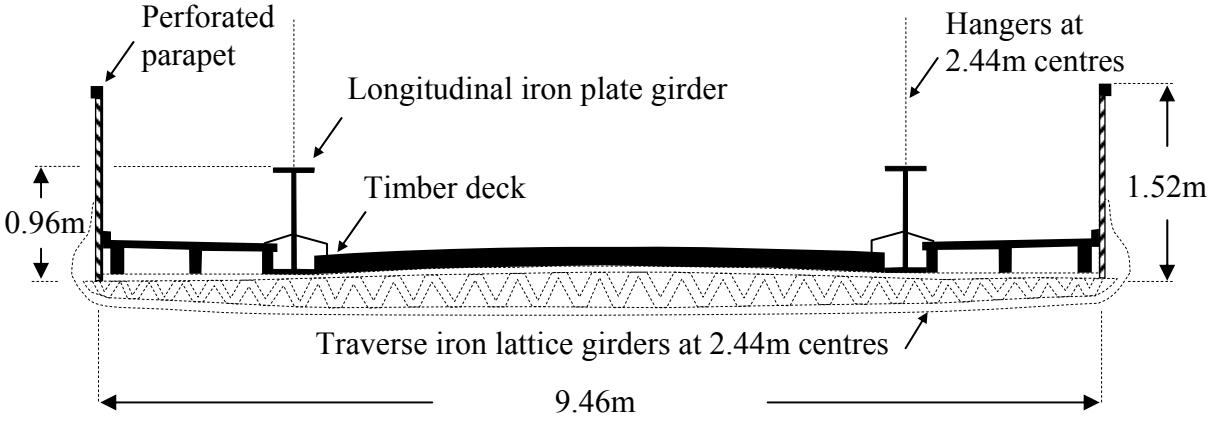

Figure 2: Sketch of the bridge cross-section.

2 WIND CHARACTERISTICS

The topography around the CSB proves to have a considerable effect on the local wind characteristics. As shown in the polar plots from both anemometers in Fig. (3), the wind speeds follow a certain trend with orientations. True North is at approximately 30˚ relative to the axes shown. The strongest winds in the absence of topographic effects are typically from about 250˚. The stronger winds as measured are aligned along the gorge and can be easily explained due to funneling of the flow in these orientations and sheltering due to the high ground near the bridge ends. It is noted that the maximum wind speed, averaged over one hour, did not exceed 16m/sec, which is a relatively low value. A histogram of 1hour average sustained wind speeds is given in Fig. (3). Maximum 1second gusts were of the order of 26m/sec for both anemometers. Generally it was observed that agreement of the wind direc-

tion and wind speed measurements for the two anemometers were strongly influenced by the wind orientation. Especially for wind speeds close to along the gorge there was an increased sensitivity giving a wide variation of the ratio between the two individual wind speed values.

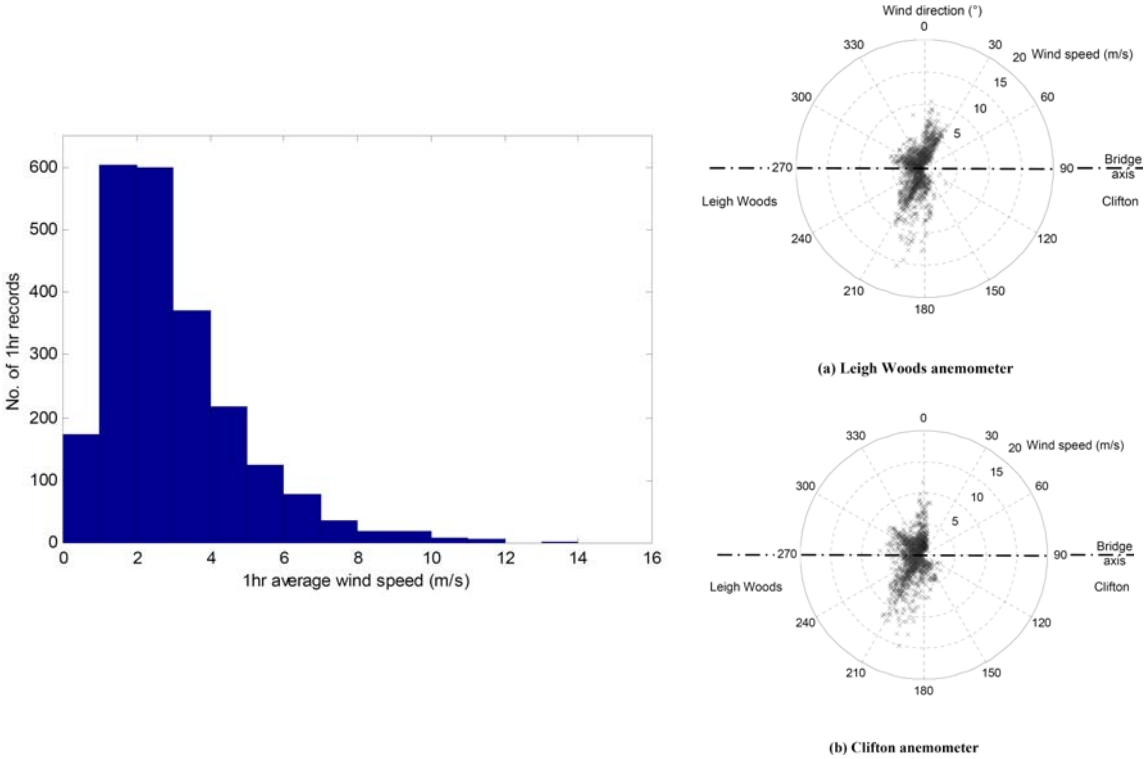

Figure 3. Left: Histogram of wind speeds during the recording period. Right: Polar plots of 1hour mean wind velocities from both anemometers.

Further the wind turbulence and angle of attack parameters were considered. For wind turbulence there was a strong dependence on wind direction and a weaker one on wind speed. High levels of turbulence were experienced, particularly for wind not along the gorge and for lower wind speeds. In winds over 8m/s, which only occurred along the gorge, approximately normal to the bridge, the mean longitudinal turbulence intensity was 21% and the mean vertical turbulence intensity 10%. The vertical and across-wind turbulence intensities followed very similar patterns to the longitudinal turbulence. For longitudinal turbulence intensities up to 40%, the across-wind turbulence was approximately equal to it and the vertical turbulence intensity approximately half of the value. These are typical of relationships between the three components of turbulence. For higher turbulence intensities measured, generally in lower wind speeds, the vertical and across-wind turbulence intensities were relatively larger.

For the vertical angle of attack there also strong dependence on the wind direction, and there were noticeable differences in the measurements from the two anemometers. The presence of the bridge itself is likely to have affected these measurements, as well as the topography of the gorge, since the anemometers were relatively close to the deck. Quite high vertical angles of attack occurred, up to approximately ±10°. (It should be noted that these values are all averaged over 1hour periods). There was no significant difference in vertical angles of attack for different wind speeds.

A final wind aspect significant for the subsequent analysis refers to its frequency components. Although traffic loading seems to be reasonably well captured by a white noise loading

approximation, the same does not hold for wind. By comparing spectral estimates deduced for various combinations of wind and traffic loading it was found that the wind loading spectra appeared as 1/*f* noise with a power exponent -8/3, thus producing a general loading spectrum approximated by a relation of the form:

$$S_{\text{load}}(f) = S_{\text{w}} f^{-8/3} + S_{\text{t}}, \tag{1}$$

where: S_{w} is a constant for a given record, being a function of the wind parameters,
f is frequency and
S_{t} is the magnitude of white noise traffic loading for the particular record.

3 RESPONSE AND MODAL PARAMETERS

3.1 Response Characteristics

Fig. (4) shows the 1hour average wind speeds over the whole monitoring period, and the corresponding Root Mean Square (RMS) vertical accelerations at the reference cross-section. The RMS amplitudes normally show a clear daily cycle with the varying traffic load, with a maximum vertical response of approximately 0.02m/s^2. By comparison it can be seen that only in wind speeds exceeding approximately 8m/s does the response noticeably exceed the maximum traffic-induced response. The maximum wind-induced acceleration measured was approximately four times the maximum traffic-induced acceleration. The torsional and lateral acceleration responses at the reference cross-section followed very similar patterns to the vertical response over the monitoring period, although the magnitudes of the responses were lower. The maximum instantaneous value of each component was found approximately 6 times the 1hour RMS value.

Dynamic displacements were calculated from the measured accelerations by double integration and it was noticed that the response is dominated by low frequency modes. The dominance of the low frequency modes is caused by the relatively higher wind loading at low frequencies and the effect of the integration, which exaggerates low frequency components. Whereas the maximum RMS acceleration due to wind loading was approximately four times the maximum due to traffic loading, in terms of displacement the maximum RMS response to wind was approximately 10 times that for traffic. This was due to the relatively greater excitation of the low frequency modes by the wind, which give the majority of the displacement.

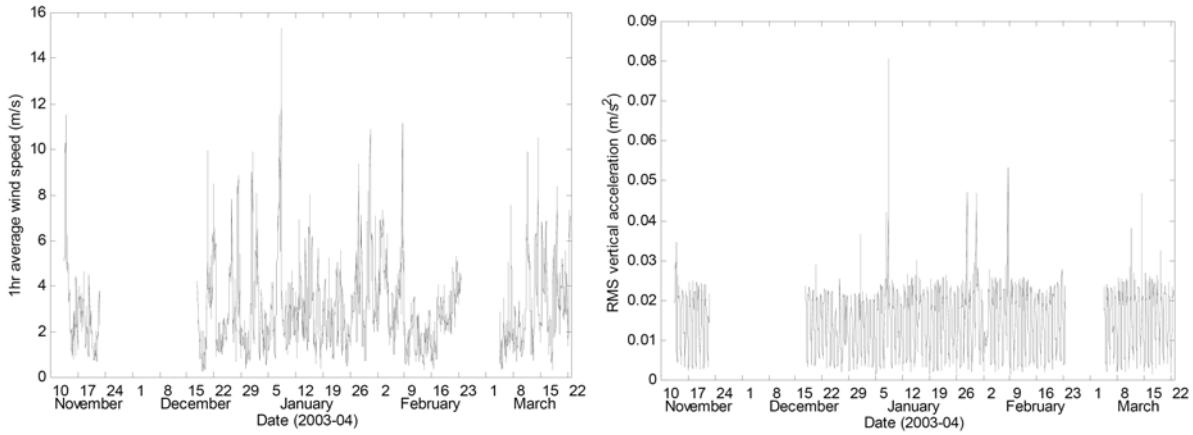

Figure 4. Left: 1hr average wind speed over the monitoring period. Right: 1hour RMS vertical accelerations at the reference location over the monitoring period.

The influence of wind loading on the measured vertical accelerations is schematically given in Fig. (5). Similar figures can be obtained for the lateral and torsional accelerations. It is apparent that growing wind speeds produce an increasing effect on the response. Scatter of results particularly at low wind speeds is largely due to varying traffic contribution. Excluding records dominated by traffic and scaling with the corresponding turbulence intensities gives a much clearer relationship to wind speed as shown on the right of Fig. (5). RMS responses are then close to power law functions of the wind speed with a power exponent of the approximate value 3.

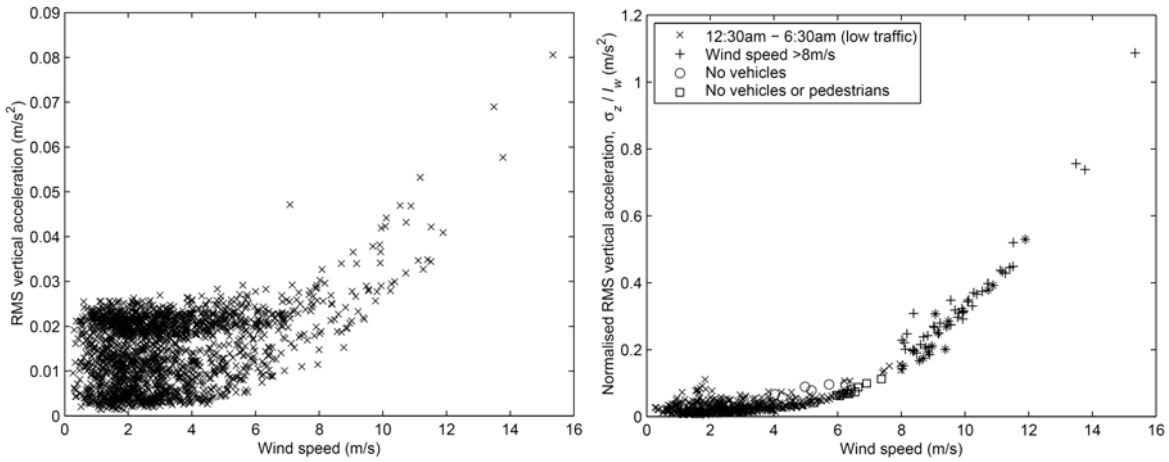

Figure 5. Left: RMS vertical accelerations in relation to wind speed for all 1hr records. Right: Scaled with turbulence intensity RMS vertical accelerations in relation to wind speed for low traffic 1hr records.

3.2 Modal Analysis

Modal parameters were calculated from the acceleration Power Spectral Densities (PSDs) using the Iterative Windowed Curve-fitting Method [7], specifically developed for the analysis of ambient vibration data since it allows for the previously specified loading spectrum. Measurements were only taken on the suspended bridge deck, but all modes inevitably involve vibrations of other parts of the structure, particularly the chains. Analysis was performed for frequencies up to 3Hz with twelve vertical, eleven torsional and four lateral modes being identified in this range, based on measurements in low wind speeds [1]. Typical PSDs for three different loading scenarios for vertical, torsional and lateral accelerations are given in Fig. (6) to present the effect of wind loading on the bridge response. The most interesting finding comprises of the close first pairs of vertical and torsional modes with frequencies of 0.293Hz and 0.356Hz respectively, which seem to couple in a potentially incipient flutter motion as can roughly be noticed in the vertical spectra in Fig. (6) and more clearly in Fig. (7).

In Fig. (7) the responses for the highest 1hour wind speed were filtered and appropriately modified (by deducting the responses from the next higher modes) to only include motion of these first two modes. The peak in the vertical PSD just over the torsional frequency is strong evidence of a coupling action. The coupling was not evident for light winds. It is also worth noting that the next pair of modes showed an equal tendency for coupling action in strong winds due to the close shape relevance and the close to unity frequency ratio. The next section discusses in more detail the identification of the CSB flutter derivatives, so as to be able to quantify the observed coupling signs.

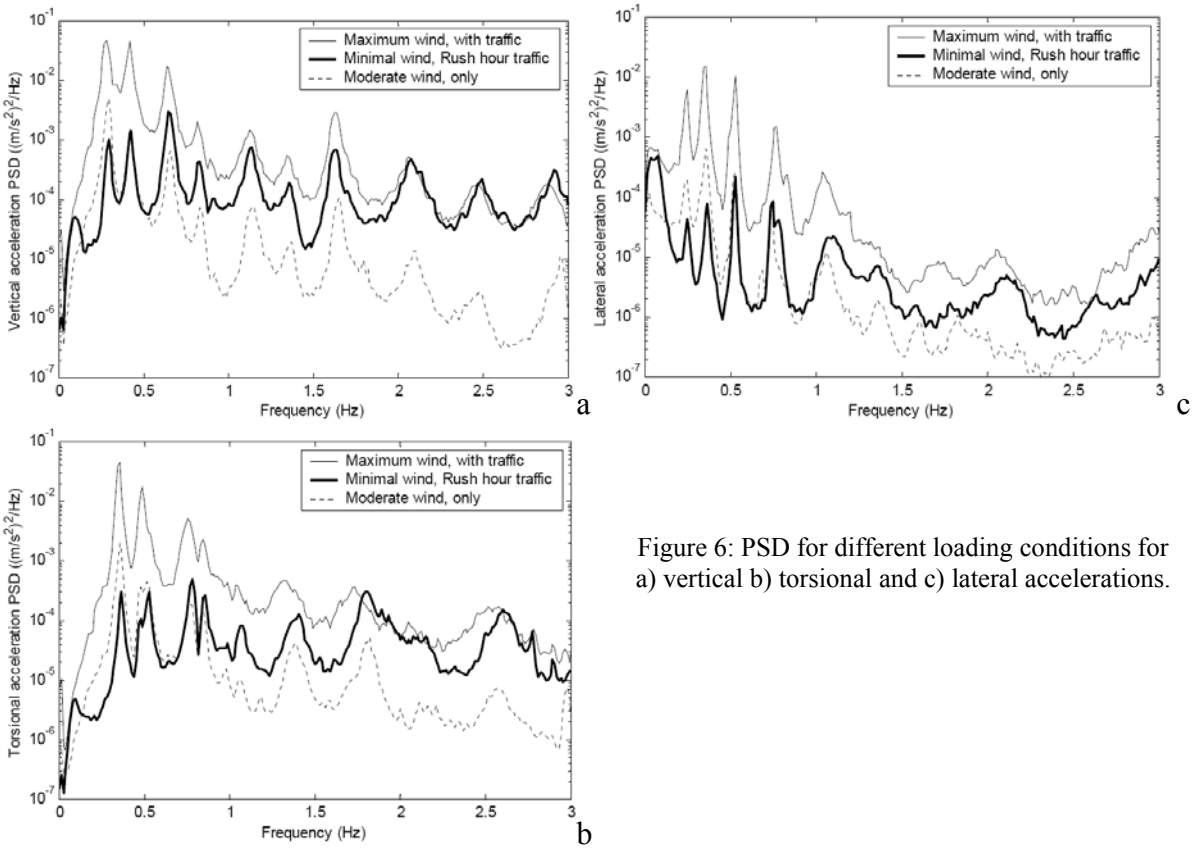

Figure 6: PSD for different loading conditions for a) vertical b) torsional and c) lateral accelerations.

4 FLUTTER DERIVATIVES

4.1 Flutter Analysis

According to the semi-empirical Selberg [8] equation for bridge sections resembling flat plates:

$$\frac{U_F}{f_{\theta 0} B} = C\sqrt{\frac{r_g m}{\rho B^3}[1-(\frac{f_{z0}}{f_{\theta 0}})^2]} \quad , \tag{2}$$

[1]

for the pair of natural frequencies described above and for m=5370kg/m, r_g=4m, ρ=1.2kg/m^3 B=9.46m and C=2 the flutter onset speed is estimated around 20m/sec, which is deemed as a very low value. This is due to the close neighbourhood of vertical and torsional modes, their shape affinity and the low mass per unit length. Although the bridge cross-section is not a flat plate and the formula for the values employed is only a first approximation, such an estimation, if approximately close to reality, could be threatening for the structural integrity of the historic bridge since it is not far beyond the operational range of wind speeds sustained in the area.

For evaluating the flutter behaviour we adopt the classical 2D formulation of Scanlan and Tomko [6] where aeroelastic forces are taken as a linear combination of the modal displacements and velocities appropriately multiplied with the so-called flutter derivatives. Namely

[1] U_F= flutter speed, B= deck width, r_g= radius of gyration, m= deck mass per unit length, C= constant depending on the mode shape similarity, ρ= air density, f_{z0} and $f_{\theta 0}$ =still air vertical and torsional frequencies.

the motion dependent lift and overturning moment L_{ae} and M_{ae} (we herein ignore the motion induced drag force D_{ae}) are given by

$$L_{ae} = \frac{1}{2}\rho U^2 B\left[kH_1^* \frac{\dot{z}}{U} + kH_2^* \frac{B\dot{\theta}}{U} + k^2 H_3^* \theta + kH_4^* \frac{z}{B} \right] , \tag{3}$$

$$M_{ae} = \frac{1}{2}\rho U^2 B^2\left[kA_1^* \frac{\dot{z}}{U} + kA_2^* \frac{B\dot{\theta}}{U} + k^2 A_3^* \theta + kA_4^* \frac{z}{B} \right] . \tag{4}$$

where U is wind speed, z vertical displacement, θ twisting and $k=\omega B/U=2\pi/U_r$ is reduced frequency, which is directly proportional to the number of oscillation cycles during the free stream flow passage over the width B. Taking on the preposition of low-level damping, as generally implied in the modelling of self-excited forces and conventional bridge flutter analysis, the flutter derivatives H_i^* and A_i^* with i=1,2,3,4 become only functions of the reduced frequency k (or equivalently of the reduced wind speed U_r), Chen [9].

4.2 Identification Method

We can assemble a state space formulation of the dynamic problem and use the Covariance Block Hankel Matrix Method (CBHM method) initially applied by Hoen et al. [10] for modal identification of offshore platforms and later modified by Jakobsen [3] to be used in the estimation of flutter derivatives, to obtain approximations of the evolution of flutter attributes. The method is founded on a Singular Value Decomposition (SVD) and an appropriate factorization of a Hankel matrix built up by covariance estimates of the displacements' time series. If y stands for displacement, z and θ in this case, then the unbiased cross covariance matrix to be used in the Hankel matrix construction is given by

$$C_{yy}(i+n,i) = C_{yy}(n) = \frac{1}{N-n}\sum y(i+n)y^T(i), \qquad n = 0,1,..,l. \tag{5}$$

where n is the number of sampling intervals for the discrete time delay $n\Delta t$, N is the number of samples in the time series, l is the maximum number of lags considered and i is a counting index. The biased estimate which only differs in the denominator N instead of N - n can be used instead with negligible differences for long time records and higher damping values. The method assumes a white noise loading to recover the assumed random loading process of wind excitation. Appropriate filtering can be used on response data to reduce artefacts introduced by the colouring of the real wind spectra with care taken on the relative filtering values of each frequency so that the real coupling effect is not altered in any way.

The decomposition of the Hankel matrix recovers all parameters of the discrete time realization. Knowing the modal stiffness and damping matrices for the in-wind and still air (pure structural stiffness and damping contributions) cases allows the separation of the flutter derivative components. The whole method relies on the choice of two parameters; the length of the individual time record N and the block dimension of the Hankel matrix defined by $S_{BHM} = l/2$. The choice of both is investigated through a sensitivity analysis together with inspection of the time evolution of the auto and cross-covariance functions.

4.3 Application to the CSB bridge

The proximity of the fundamental vertical and torsional modes, as presented in Fig. (7), seems to encourage some coupling action, which can potentially be recognized as classical flutter. The PSDs in Fig. (7) imply some non-negligible values of H_2^* or H_3^* flutter derivatives since the coupling contribution is evidently located in the vertical PSD at the torsional

frequency. For the flutter derivative identification there were used in one case the recorded acceleration data and in another the double integrated displacements evaluated from the accelerations in hand. Both cases produced identical results.

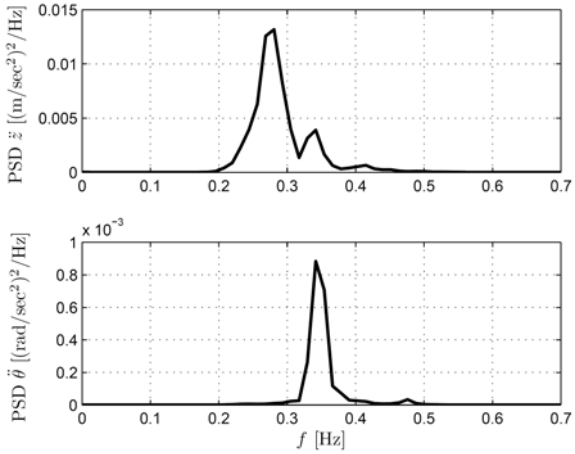

Figure 7: PSDs of filtered data for first vertical and torsional modes. The coupling action is evident in the vertical PSD for a wind speed of around 16m/sec.

For selection of the two foresaid identification parameters a range for time records from 10 minutes to 1 hour and for the covariance function length, lags in the range of 20 to 80 seconds were used. Example covariance functions, for moderately strong wind, are plotted against time in Fig. (8). As previously demonstrated by Jakobsen [11], the sensitivity in the chosen value of maximum time lags is strongly influenced by the wind speed. Higher wind speeds usually require a shorter portion of the covariance function for accurately reproducing the 2degree of freedom interrelation. For our case an optimum set of values was found to be the combination of 15minute records (N = 11264) with Hankel matrix block dimension S_{BHM} = 250 (20sec) with only weak sensitivity on changing S_{BHM}, probably due to the small magnitude of wind speeds.

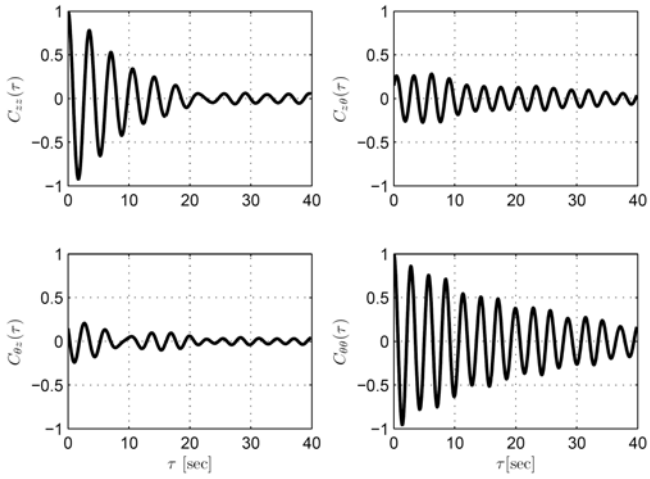

Figure 8: Covariance functions for the combined two degrees of freedom plotted against time.

Results for the CSB flutter derivatives are given in Fig. (9). Where possible, data are compared with available wind tunnel results of other deck cross-sections. Sign conventions for aerodynamic forces were as in Scanlan and Tomko [6].The observed deviations from the ex-

pected zero values for still air conditions should be attributed mainly to lack of precise estimates of structural damping and stiffness and to the relatively high distorting action of traffic on the response for low wind speeds. A sensitivity analysis on the measured wind characteristics, such as the turbulence and the angle of attack, proved not to be able to reproduce a clear picture of their effect. The identified trends remained unaltered but data were insufficient for quantifying the impact of the characteristics.

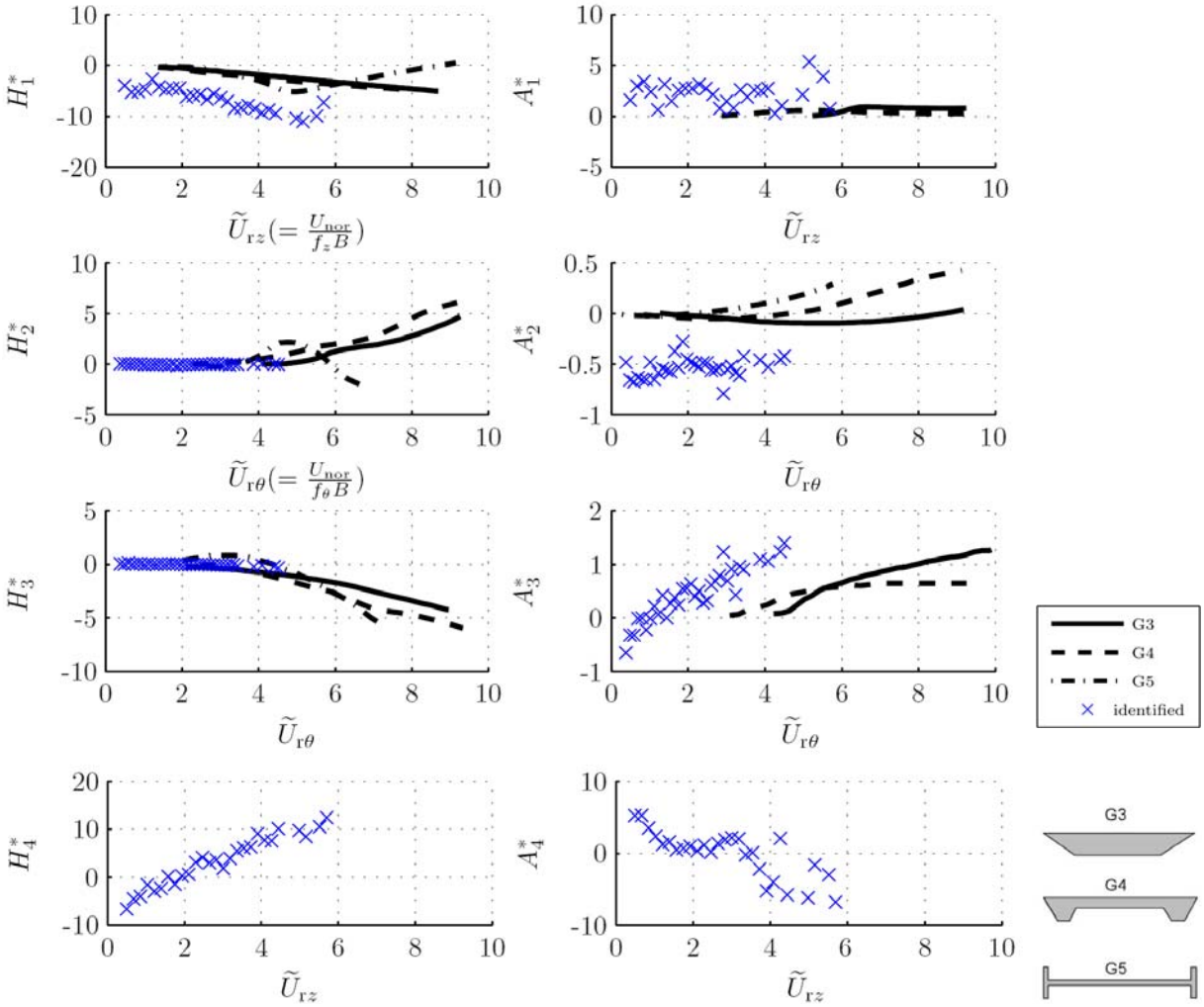

Figure 9: Flutter derivatives of Clifton Suspension Bridge from full scale data, compared with wind tunnel extracted flutter derivatives for various cross-sections (after Scanlan and Tomko [6]). Where a line is not given the corresponding flutter derivative is negligible. Identified values correspond to averaged identified values. The reduced wind speed variables used in the horizontal axes are evaluated in terms of the normal wind speed.

Although the identified flutter derivatives are noisy, unsurprisingly for full-scale ambient data, some trends are apparent. The results indicate that, within the range of wind speeds recorded (maximum 16m/sec), the bridge is not susceptible to vertical or torsional flutter (so called "damping-driven flutter" as presented by Matsumoto [12]), which was the actual reason for the famous Tacoma Narrows Bridge collapse. This is due to having negative H_1^* and A_2^* which do not reverse the initial still air sign of the damping. However, H_1^* apparently shows a positive gradient near the highest wind speed recorded, suggesting it could become positive for higher wind speeds, possibly leading to flutter. This trend persists regardless of the selected identification parameters (N and S_{BHM}), indicating it is not due to numerical errors, although the last few points in the figure are from averages over few records, so their accuracy

is limited. If confirmed, the effect of possible positive H_1^* (i.e. negative damping) could provide a feasible explanation for the occasional observations of large vibrations of the bridge in strong winds.

The H_2^* and H_3^* derivatives, which control the coupling from torsional to vertical motion, have small values. However at the higher wind speeds there is a slight negative trend in H_3^*, in line with the curves for other bridge profiles, which potentially explains the previously illustrated coupled spectra in Fig. (7). Derivatives H_4^* and A_4^* have proved to be of less importance for the flutter phenomenon, but they are presented here for completeness of presentation and they do exhibit trends. The evolution of H_4^* reflects the reduction of vertical natural frequency with increasing wind speed, although this could alternatively be due to an amplitude dependence rather than the wind. Similarly A_3^* illustrates the reduction in the torsional natural frequency.

Some of the derivatives in Fig. (9) appear to have an offset for still-air wind conditions. This was also encountered in previous treatises, Jakobsen [3], and should here be mostly appointed to parameters such as the traffic distorting action, abnormalities in the mass distribution, and slight inaccuracies in the still-air structural matrices considered. For any additional quantitative considerations, including estimating the critical flutter wind speed, data inclusive of higher wind speeds are needed.

5 CONCLUSIONS

The measured full-scale response of the Clifton Suspension Bridge has been analyzed and flutter derivatives were extracted using an elaborate stochastic identification method. It has been shown that ambient vibration identification techniques can yield sensible results for full-scale structures although such a task may seem formidable. Trends in some of the flutter derivatives have been identified. For the historic bridge with more than 140 years of life, there is no cause for concern within the range of wind speeds recorded (up to 16m/sec). However, there is some indication of an adverse trend in H_1^* (and some coupling of torsional and vertical motion) which could possibly lead to flutter in higher wind speeds, but this is based on uncertain data. Recordings in stronger winds would be valuable to understand the bridge behaviour more fully. The Covariance Block Hankel Matrix Method was tested for a range of different record and Hankel matrix lengths. Thus it allowed a valuable insight, which can be used in further assessments of monitoring potentially problematic large engineering structures.

AKNOWLEDGEMENTS

The authors gratefully acknowledge the support of the Clifton Suspension Bridge Trust for the site tests and the support of EPSRC for the analysis under Macdonald's Advanced Research Fellowship and associated grant.

REFERENCES

[1] J. H. G. Macdonald. Pedestrian-induced vibrations of the Clifton Suspension Bridge, UK. *Proc. ICE: Bridge Engineering*. **161** (BE2), 69-77, 2008.

[2] J. H. G. Macdonald. Evaluation of buffeting predictions of a cable-stayed bridge from full-scale measurements. *J. Wind Eng. Ind. Aerodyn.*, **91**, 1465-1483, 2003.

[3] J. B. Jakobsen. Fluctuating wind load response of line-like engineering structure with emphasis on motion-induced wind forces. PhD Thesis. Department of Structural Engineering, University of Trondheim, Norway, 1993.

[4] J. B. Jakobsen and G. L. Larose. Estimation of aerodynamic derivatives from ambient vibration data, 10th Int. Conf. Wind Engineering, 837-844, 1999.

[5] C. Costa and C. Borri. Full-scale identification of aeroelastic parameters of bridges, 12th Int. Conf. Wind Engineering, Cairns, Australia, 799-806, 2007.

[6] R. H. Scanlan and J. J. Tomko. Airfoil and bridge flutter derivatives. *J. Eng. Mech. Div.*, ASCE, **97** (EM6), 1717-1737, 1971.

[7] J. H. G. Macdonald. Identification of the dynamic behaviour of a cable-stayed bridge from full-scale testing during and after construction. PhD Thesis. Department of Civil Engineering, University of Bristol, UK, 2000.

[8] A. Selberg. Aerodynamic effects on suspension bridges. Int. Conf. Wind Effects on Buildings and Structures, Vol. II, 462-479, 1963.

[9] X. Chen. Improved Understanding of Bimodal Coupled Bridge Flutter Based on Closed-Form Solutions. *ASCE J. Structural Engineering*, **133** (1), 22-31, 2007.

[10] C. Hoen, T. Moan and S. Remseth. System identification of structures exposed to environmental loads, 2nd European Conference on Structural Dynamics, EURODYN'93, Trondheim, Norway, 1993.

[11] J. B. Jakobsen M. G. Savage and G. L. Larose. Aerodynamic derivatives from the buffeting response of a flat plate model with stabilizing winglets, 11th Int. Conf. Wind Engineering, Lubbock, Texas, 673-680, 2003.

[12] M. Matsumoto, Y. Koboyashi and H. Shirato. The influence of aerodynamic derivatives on flutter. *J. Wind Eng. Ind. Aerodyn.*, **60**, 227-239, 1996.